Journal of Geomatics Vol. 13, No. 2, October 2019

Carbon stock assessment in different land use sectors of Ziro valley, Arunachal Pradesh using geospatial approach

Bordoloi R[*,1], Das B[1], Yam G[2], Deka S[1], Tripathi OP[1]
[1]Department of Forestry, NERIST (Deemed to be University) Arunachal Pradesh
[2]Department of Zoology, Rajiv Gandhi University, Rono Hills, Arunachal Pradesh
*Email: ritashree.100@gmail.com

(Received: Jan 05 2018; in final form: Oct 11, 2019)

Abstract: Land use change particularly vegetation change is considered a major factor in reshaping the distribution of carbon stocks. The rapid changes in prevailing land use types tends to reduce forest cover thereby reducing the potential of carbon capture and storage. The study aims to calculate the amount of carbon stock in dissimilar land use of Ziro Valley in Arunachal Pradesh. Altogether 24 (0.1ha each) permanent plots were established under different land use viz; mixed forests, pine forests and agricultural land. To study the tree biomass and carbon under selected landuse, non-destructive biomass sampling approach was used. A total 102 species were recorded during the sampling. Species such as *Pinus wallichiana, Castonopsis indica, C. hystrics, Rhododendron hodgsonii, Elaeocarpus rugosus, Quercus myrsinifolia* were among the most frequent species. The stand density ranges from 440 to 770 stems/ha in the forest area. Species-specific volume equations were used to calculate the above ground biomass (AGB). The AGB recorded from the mixed forests ranged from 140.55 t/ha to 316.18 t/ha and in pine forests it was recorded 102.04 to 184.46 t/ha. The AGB recorded at shrub layer in the mixed forests varied from 4.71 to 7.29 t/ha and it was 5.38 to 13.46 t/ha in pine forests. The total carbon calculated for the mixed forests including soil organic carbon (SOC) was 131.35 tonnes /ha to 309.12 t/ha and it was recorded 129.66 t/ha to 203.02 t/ha in pine forests. The total soil carbon recorded in the agricultural field ranges from 11.53 t /ha to 61.45 t /ha. The present study reveals how the conversion of forest in to agriculture land will minimize the carbon capture potential of the forest land use. The different satellite data based modelling approach was also applied in this study to predict overall carbon stock of the study area.

Keywords: Carbon, Land use, Vegetation, Biomass, Pine forest, mixed forest.

1. Introduction

Terrestrial ecosystems are the storehouse of carbon reserved in the form of living biomass, litter, humus and soil organic matter, play a significant role in nutrient cycling including carbon cycle. Spatially and temporally variant carbon sources and sinks were also seen in Indian terrestrial ecosystem due to its diverse climate system; diversified by various land use distribution and other management practices. In terrestrial ecosystems, the carbon uptake takes place in both vegetation and soils. Soil contains about 75% of the global carbon and plays a vital role not only in crop production but also in managing carbon concentration in atmosphere (Schlesinger, 1999). Forest vegetation is important component of land cover and plays important role in carbon dynamics. The diverse structural composition of the forests, and other biotic disturbances and extractions of the trees contributes significantly in carbon cycle thereby shaping Global carbon resources (Bhat and Ravindranath, 2011). Land use changes tend to immediately bring disturbances in soil and ambient environment. The annual carbon fluxes to the atmosphere from land cover alterations aids in defining the global carbon budget (Le Quere et al., 2015) and offers the prospective to land administration in understanding the removal of carbon from atmosphere (Houghton et al., 2015). Arneth et al. (2017) reported historical CO_2 emissions from the terrestrial ecosystem resulted from land use changes and regarded to be perhaps larger than that assumed. Quantification of carbon stocks is very complex and in order to understand the complexity of the carbon cycle and its linkages, estimations are done through ground truth approach and carbon dynamics simulation through geospatial techniques. Remotely sensed data coupled with geospatial approaches plays a noteworthy role in present scenario in mapping and monitoring of land cover in shorter time span as compared to ground based approach (Jensen, 1986; Treitz and Rogan, 2004). Remote sensing images have revealed high correlation between spectral bands and vegetation which is in general the most important for estimation of above ground biomass (AGB) for large area (Nelson et al., 2000; Foody et al., 2003). The above technology is also capable in collecting data for areas which cannot be accessed due to undulating topography and other site variability. Keeping in mind the limited empirical analysis of land use changes in the context of major land cover C dynamics in the state of Arunachal Pradesh, the proposed objectives was carried out to calculate carbon stocks in major land use i.e., mixed forests, pine forests and agricultural land in the Ziro valley.

2. Study area

The Ziro valley is situated in Lower Subansiri district of Arunachal Pradesh (93º45′35.54′′ to 94º01′01.83′′ E longitudes and 27º25′25.36′′ to 27º38′22.8′′ N latitudes) having altitudinal range of 1,524 to 2,900 m asl. The Lower Subansiri district is bounded by Kurung Kumey and Upper Subansiri districts in the North, in the East by West Siang and Upper Subansiri districts, and Papum Pare district and the state of Assam to the South (Figure 1). The Ziro valley is frequently called as the Apatani plateau. The geographical coverage of study area is 3,460 km^2 of which about 33 km^2 areas is under agricultural lands and remaining area is either under forest cover, plantations or settlement

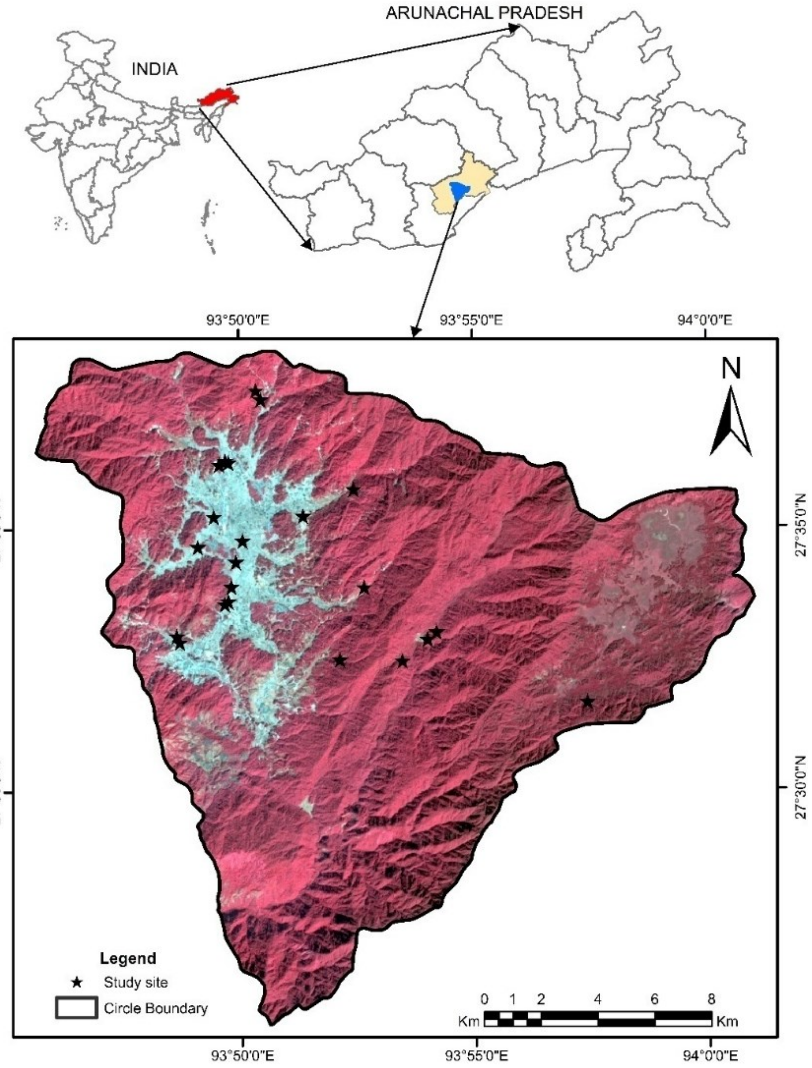

Figure 1: Location map of the study area

The area experiences warm subtropical to temperate climate. The Ziro valley experiences four seasons in a year i.e., cool winter, pre-monsoon, monsoon and post-monsoon seasons. Least temperature is recorded amid December and January and greater temperature amid summer in the July and August (Figure 2). The normal yearly precipitation of the study area for the year 2017 was recorded with low (5.76 mm) to high (496.51 mm) precipitation amid the May-July. The relative humidity remains high 78.16 % throughout the year, with the exception of winters when it slightly goes down (Figure. 2). The LULC map of the Ziro valley was prepared using LANDSAT OLI, 2017 satellite data and classified map is presented (Figure 3). The physiography of the study area had supported the rich vegetation having broad variety of forest resources.

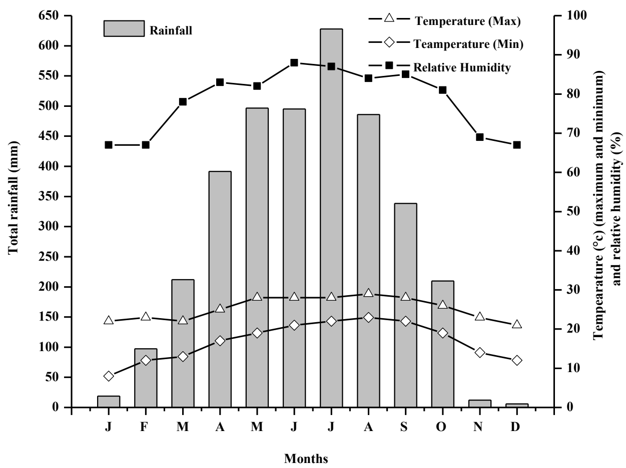

Figure 2: Climatogram of the study area

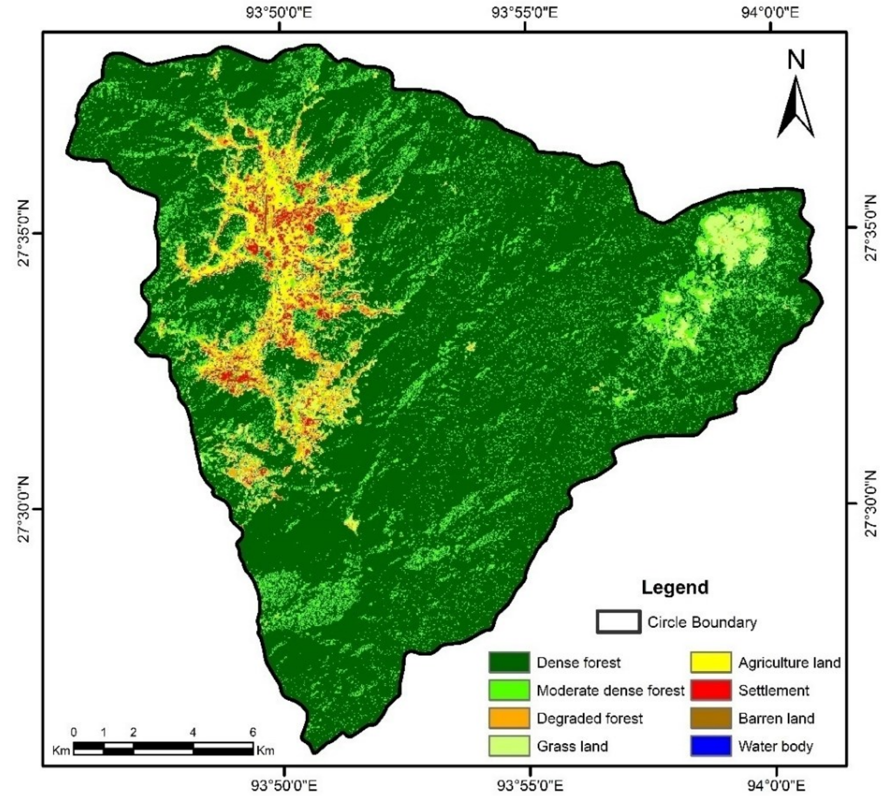

Figure 3: Land use land cover map of the study area

3. Data used and methodology

To measure the biomass, plots of 30m x 30m were sampled randomly from selected land cover and land use. The number of plots selected for all landuse types were primarily depending on the distributions/coverage and the variability in the carbon content in account. For the major land use, mixed forests, pine forests and agricultural lands were selected. The individual trees per ha, basal area and biomass (Mg/ha) were computed based on the sampled data. The AGB was estimated using volume equation (Appendix-I) of Forest Survey of India (FSI, 1996). The biomass of the under-storey (diameter less than 10 cm) were analysed in the sub plots of 5 m × 5m following NRSC-ISRO field manual and herb species were calculated using harvest methods (fresh weight basis) in sampled plots of 1m x1m within the nested plot of 30 m × 30 m. It was assumed that the above ground components have 55 % of Carbon (Mac Dicken, 1997). Random samples of soil from each 30m x 30m plot were collected in replicates. The soils were sampled to a depth of 45 cm and separated into different layers i.e., 0-15, 15-30 and 30-45 cm during the soil sample collection. Soil bulk density was measured using soil corer method as described by Anderson and Ingram (1993). Below ground biomass was calculated considering factor 0.29 of the AGB (IPCC 2005). Soil organic carbon was determined using the Walkley and Black (1934) method. The SOC content was calculated for bulk density and summed to estimate total SOC content.

3.1 Remote sensed data

Remote sensing permits to study the possessions and procedures of land uses and their temporal variability at different dimensions (Prince and Goward, 1995; Running et al., 2000). The Landsat OLI image (5 Dec, 2017; Path 135, Row 41) of the study area was collected to calculate various vegetation indices. The collected initial satellite data for each OLI band were radiometrically calibrated to top of atmosphere surface reflectance. Further, processing of images involved several image processing techniques such as geometric correction, mosaicking and extraction of study area. Radiometric correction of each band was done through ERDAS imagine 9.1 following LANDSAT 8 user handbook. After radiometric correction all the images were re-projected to Universal Transverse Projection system followed by delineation of study area. Land use and land cover map was prepared using unsupervised classification through ERDAS imagine 9.1.

DN to Radiance Conversion

Images are processed in units of absolute radiance using 32-bit floating point calculations. These values are then converted to 16-bit integer values in the finished level 1 product. These values can then be converted to spectral radiance using the radiance scaling factors provided in the metadata file:

$$L\lambda = M_L * Qcal + A_L$$

Where: $L\lambda$ = Spectral radiance (W/(m2 * sr * µm)), M_L = Radiance multiplicative scaling factor for the band , A_L = Radiance additive scaling factor for the band , Qcal = Level 1 pixel value in DN.

Table 1: Vegetation indices used in current study

Vegetation Indices	Expression	Author
NDVI	$\mathrm{NDVI} = \frac{\mathrm{NIR} - \mathrm{R}}{\mathrm{NIR} + \mathrm{R}}$	Rouse et al. (1974)
TVI	$\mathrm{TVI} = \sqrt{\frac{NIR - R}{NIR + R}} + 0.5$	Deering et al. (1975)
SAVI	$\mathrm{SAVI} = \frac{\mathrm{NIR} - \mathrm{R}}{\mathrm{NIR} + \mathrm{R} + \mathrm{L}}(1 + \mathrm{L})$	Huete (1988)

Top of Atmosphere Reflectance

Similar to the conversion to radiance, the 16-bit integer values in the level 1 product can also be converted to Top of Atmosphere (TOA) reflectance. The following equation is used to convert level 1 DN values to TOA reflectance:

$$\rho\lambda' = M\rho * Qcal + A\rho$$

where:

$\rho\lambda'$: Top-of-Atmosphere Planetary Spectral Reflectance, without correction for solar angle. (Unit less)

$M\rho$: Reflectance multiplicative scaling factor for the band .

$A\rho$: Reflectance additive scaling factor for the band

Qcal l: Level 1 pixel value in DN

Note that $\rho\lambda'$ is not true TOA Reflectance, because it does not contain a correction for the solar elevation angle. This correction factor is left out of the level 1 scaling at the users' request); some users are content with the scene-centre solar elevation angle in the metadata, while others prefer to calculate their own per-pixel solar elevation angle across the entire scene. Once a solar elevation angle is chosen, the conversion to true TOA Reflectance is:

$$\boldsymbol{\rho\lambda} = \boldsymbol{\rho\lambda'}/\mathbf{sin}(\boldsymbol{\theta})$$

where:

$\rho\lambda$ = Top-of-Atmosphere Planetary Reflectance (Unitless)

θ = Solar Elevation Angle (from the metadata, or calculated).

*Above ground biomass**:** remote sensing approach*

The current study emphasized three mostly used vegetation indices connected with satellite image change detection and biomass estimation was used. Vegetation indices are the best indicator of greenness of vegetation canopy and hence used to predict the above ground biomass estimation and prediction (Xue and Su, 2017) Almost all vegetation indices derived by the taking ratio of Near Infrared band (NIR) and Red band (R). The current study comprises indices (Table 1) of the normalized difference vegetation index (NDVI), which is the ratio of contrasting reflectance between the maximum absorption of the red wavelength and maximum reflectance of the infrared wavelength (Powel et al., 2010) and its value ranged between -1 to 1, the transformed vegetation index (TVI), which is the same as NDVI but values are always positive as addition of factor of 0.5 to absolute of NDVI and its value ranged in 0 to 1, the soil adjusted vegetation index (SAVI), which is similar to the NDVI but illuminates the soil brightness effect (Richardson and Wiegnad, 1977).

Spectral modeling of carbon stock estimation and prediction using satellite derived vegetation indices have been performed in the present study. The linear regression analysis done between fields based total carbon which was calculated by taking carbon observed in different plant component (AGB, BGB, herb, shrub and soil carbon) and vegetation indices.

4. Results and discussion

The results show the variations in biomass between the mixed forests and pine forests. Stand density, basal area and biomass showed noteworthy variation between the land use types. Altogether, 102 species were recorded from the present study area. Species like *Pinus wallichiana, Castonopsis indica, C. hysterics, Rhododendron hodgsonii, Elaeocarpus rugosus, Quercus myrsinifolia* were among the most frequent species. Based on the study it was observed that the basal area (m^2 /0.1ha) of the woody species ranged from 3.68 to 8.08 in the mixed forests and it was 2.60 to 4.45 in the pine forests. The stand density ranges from 440 stems/ha to 770 stems/ha in the mixed forests and 450 stems/ha to 600 stems/ha in the pine forests.

The volume equations were fitted to the data using diameter at breast height (dbh), height (H) and the combined variable dbh^2H as explanatory variables for the woody species. Species-specific biomass estimation was done for each plot. Biomass per plot (0.1 ha) was estimated by summing up the species present in the respective plots. The AGB ranges from 140.55 t/ha to 316.18 t/ha in the mixed forests whereas it varied from 102.04 to 184.46 t/ha in the pine forests. The findings of the present study are in conformity with the values reported of 7.25 t/ha to 287.047 t/ha in different vegetation types (Devagiri et al., 2013), 6.39 t/ha to 215.57 t/ha in tropical forest ecosystems (Khangar and Hirandhede, 2016). Evaluation of total AGB in the different land use types showed that the total AGB was higher in mixed forests as compared to pine forests and agricultural land. The biomass (t /ha) of the under-storey shrubs ranged from 6.07 to 9.40 whereas for herbs it ranged from 0.46 to 0.74 in the mixed forests on the other hand for plantation it was recorded 6.94-17.36 under-storey shrubs and 0.17-0.27 for herbs. The field-based findings showed a positive relation (R^2=0.94) between the basal area and woody species biomass. The overall allocation of SOC also varied amongst the three landuse types. The highest proportion of SOC content was deposited in the surface layer than the sub surface layer. The average total SOC content in the mixed forests was 29.63 t/ha, 50.27 t/ha in the pine forests and 31.10 t/ha in the agricultural lands. The carbon stock sum of AGBC and SOC varied significantly over land use types. It ranges from 131.35 t/ha to 309.12 t/ha in mixed forests followed by 129.66 t/ha to 203.02 t/ha in pine forests and 11.53 t/ha to 61.45 t/ha in agricultural lands.

4.1 Spectral modelling of carbon stock

Satellite based biomass estimation of the study area was done through vegetation indices. NDVI values range between 0.08 to 0.42 among the sampled plots, 0.92 to 1.26 for the TVI, 0.12 to 0.62 for SAVI in the present study. Das et al. (2017) had reported NDVI value of 0.26 and SAVI value of 0.70 from different land use sectors of Arunachal Pradesh. To apprehend the relationship linear regression analysis was carried out between AGB and satellite derived different vegetation indices. The coefficient (R^2) of regression model between biomass and different vegetation indices were presented in Table 2 and the spatial variability map of selected land use types of the study area is given in figure 4.

Table 2: Coefficient for R^2 for biomass and different vegetation indices

Vegetation Indices	Equation	R^2
NDVI	Y = 685.57x – 23.262	0.75
TVI	Y = 432.89x – 282.82	0.41
SAVI	Y = 460.81x – 28.433	0.79

*Where x denotes the NDVI and Y denotes AGB

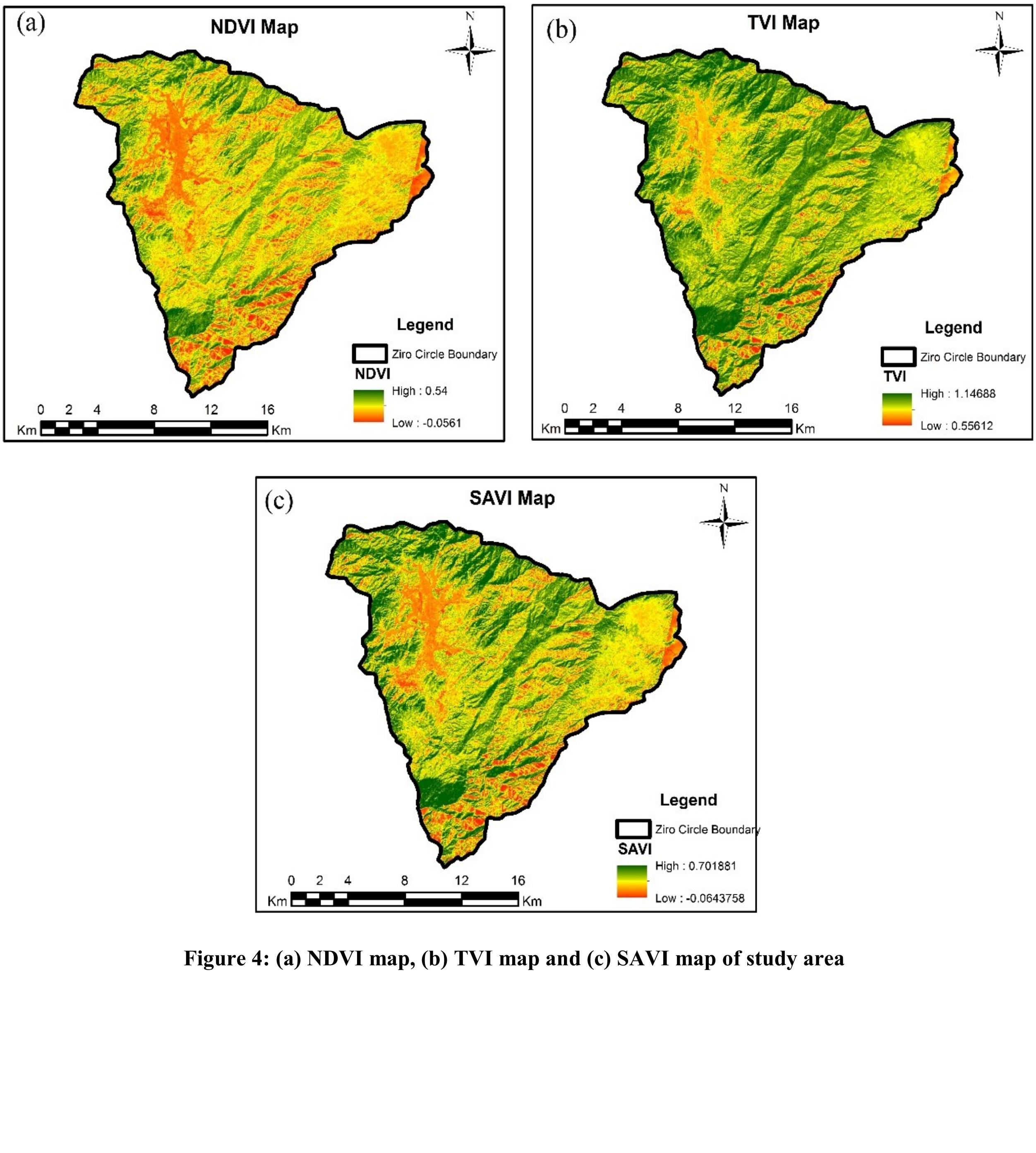

Figure 4: (a) NDVI map, (b) TVI map and (c) SAVI map of study area

The coefficient (R^2) value observed is 0.75 for NDVI, 0.41 for TVI and 0.79 for SAVI. The R^2 value observed for three vegetation indices was compared with values reported by different researchers around the world. Foody et al. (2003) had reported lower R^2 value of 0.082, 0.009 and 0.099, respectively from the Thailand, Brazil and Malaysia using Landsat TM satellite data than the values observed in the current studies. The R^2 value was also reported to be lower ($R^{2=}$ 0.046) by Zhou (2014) from South eastern Bangladesh using Landsat ETM+ bands. Rahman et al. (2008) had also reported the lower R^2 (0.138) value for NDVI. The R^2 value (0.51) reported by Mynard et al. (2007) found to be higher than the values of current study. Redowan et al. (2015) had also reported higher R^2 (0.768) value than current research. The R^2 value for TVI has very low relationship between biomass and TVI. The R^2 (0.173) value for TVI was reported by Rahman et al. (2008) from South eastern Bangladesh using Landsat ETM+ bands were lower than present observation. The higher R^2 value (0.639) was reported by Redowan et al. (2015) for Kahdimanagr national park, Bangladesh. The R^2 value ranged between 0.46 and 0.86 for south western part of Karnataka (Devagiri et al., 2013). The R^2value computed for SAVI is higher than the R^2value 0.52 reported by Zhou (2014). Ullah et al. (2012) had also studied the relationship between green biomass and SAVI and reported R^2 value (0.54) which is lower than the values observed in current study. Maynard et al. (2015) modelled the AGB using vegetation indices and reported the R^2 value of 0.51 for SAVI while in other study it was reported to be 0.029 by Rahman et al. (2008).

Though NDVI is widely used vegetation indices for biomass estimation but it showed low R^2 values in current study. NDVI has the draw backs of light scattering due to aerosols present in atmosphere which affects the biomass estimation (Ben-Ze'ev, et al., 2006). There is no significant difference in NDVI and TVI as both indices have same drawbacks. Also these two indices only use two bands (NIR and Red). In TVI, the values always show positive values and sometimes it goes beyond 1. SAVI perform better than former two indices, as it considers the soil brightness effect and correction factor was added to this which minimizes the error which was observed in NDVI.

4.1.1 Biomass and carbon stock prediction

The current study revealed that soil adjusted vegetation index (SAVI) have better relationship with the carbon stock. The best fit regression model Y = 460.81x – 28.433 (R^2 = 0.79) was used to predict carbon stock per sample plot (Figure 4). The predicted carbon stock was summed up and converted into stock per hectare. The predicted carbon stock for the study area was 118.79 t ha^{-1}. However, the carbon stock predicted for mixed forest was 177.43 t ha^{-1}, 169.23t ha^{-1} for Pine forest and it was 31.10 t ha^{-1} for paddy field. Devagiri et al. (2013) reported carbon stock of 3 Mt (mean carbon density of 33 t ha^{-1}) from Hassan district of Karnataka. Bhat et al. (2003) reported total carbon density (TCD) from 131.86 $Mgha^{-1}$ to 460.89 $Mgha^{-1}$, which indicates that the carbon density of forests reduces with increasing elevation in forest of Uttar Kannad in Western Ghats (Figure 5).

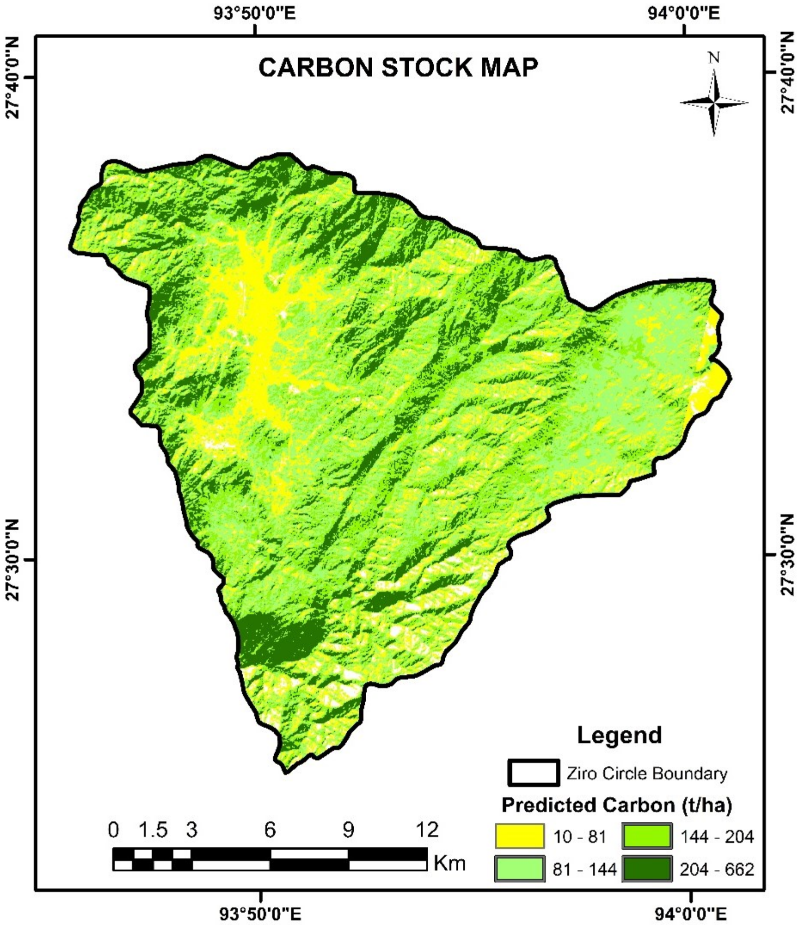

Figure 5: Predicted carbon stock for the study area

5. Conclusions

In the present study, the field based findings of the total carbon stock in the mixed forests was estimated 195.81 t/ha, it was estimated 162.26 t/ha in the pine forests and it was estimated 31.10 t/ha in agricultural lands whereas, the remote sensing based findings predicted carbon stock of the overall land use types of the study area to be 118.79 t/ha which is quite comparable with the field based findings.The difference in the biomass estimations between the observed values and predicted values might be due to the changes in the crown density and phenological conditions of vegetation types existing in the study area.This type of studies will be more successful if they are integrated with socioeconomic, ecological and political objectives for biodiversity conservation and biomass based livelihood enhancement opportunities to use forests as a part of CO_2 emission control strategy.

Dedication

This paper is dedicated to our beloved teacher Late Prof. R.S. Tripathi.

References

Anderson, J. M. and J. S. I. Ingram (1993). Tropical soil biological and fertility: a handbook of methods.

Arneth A., S. Stich, J. Pongratz, B.D. Stocker, *et al.,* (2017). Historical carbon dioxide emissions caused by land-use changes are possibly larger than assumed. Nature Geoscience, 10(2), 79–84

Ben-Ze'ev, E., A. Karnieli, N. Agam, Y. Kaufman, and B. Holben (2006). Assessing vegetation condition in the presence of biomass burning smoke by applying the Aerosol-free Vegetation Index (AFRI) on MODIS images. International Journal of Remote Sensing, 27(15), 3203-3221.

Bhat, D. M., K. S. Murali and N. H. Ravindranath (2003). Carbon stock dynamics in the tropical rainforests of Uttar Kannada district, Western Ghats, India. International Journal of Environment and Pollution, 19(2), 139-149.

Bhat, D.M. and N. H. Ravindranath (2011). Aboveground standing biomass and carbon stock dynamics under a varied degree of anthropogenic pressure in tropical rain forests of Uttara Kannada district, Western Ghats, India. Taiwaniam 56(2), 85-96.

Das, B., S. Deka, R. Bordoloi, P. K. Pandey, L. B. Singha and O. P. Tripathi (2017). Rapid assessment of above ground biomass in forest of Papum Pare district of Arunachal Pradesh: a geospatial approach, Malaya Journal of Biosciences,4(2), 48-55.

Devagiri, G. M., S. Money, S. Singh, V. K. Dadhwal, P. Patil, A. Khaplek, A. S. Devakumar and S. Hubballi (2013). Assessment of above ground biomass and carbon pool in different vegetation types of south western part of Karnataka, India spectral modelling. Tropical Ecology, 54(2), 149–165

Foody, G. M., D. S. Boyd and M. E. J. Cutler (2003). Predictive relations of tropical forest biomass from Landsat TM data and their transferability between regions. Remote Sensing of Environment, 85(4), 463–474.

FSI. 1996. Volume Equations for Forests of India, Nepal and Bhutan. Forest Survey of India, Ministry of Environment and Forests, Govt. of India, Dehradun

Houghton, R.A., B. Byers and A.A. Nassikas (2015). A role for tropical forests in stabilizing atmospheric CO2, Nature Climate Change, 5, 1022–1023.

IPCC, G.L (2005). Agriculture, Forestry and Other Land Use. IPCC Guidelines for national greenhouse gas inventories.

Jensen, J.R. (1986). Digital Image Processing. Prentice-Hall: New Jersey.

Khangar, H, and D.K. Hirandhede (2016). Studies on above ground biomass (AGB) for assessing vegetation carbon pool in tropical forest ecosystem of central India. International Journal of Pharmaceutical Sciences and Research, 7(11), 4588-91.

LANDSAT 8 (L8) Data Users Handbook Version 1.0 June 2015. (2015), 8(June).

MacDicken, K.G. (1997). A guide to monitoring carbon emissions from deforestation and degradation in developing countries: An examination of issues facing the incorporation of REDD into market-based climate policies. Resource for Future, Washington DC, 84.

Maynard, C. L., R. L. Lawrence, G.A. Nielsen and G. Decker (2015.). Modeling Vegetation Amount Using Bandwise Regression and Ecological Site Descriptions as an Alternative to Vegetation Indices, GIScience &Remote Sensing, (1), 68-81.

Nelson, R.F., D.S. Kimes, W.A. Salas, and M. Routhier (2000). Secondary forest age and tropical forest biomass estimation using Thematic Mapper imagery. Bioscience, 50, 419–431.

Prince, S.D. and S.N. Goward (1995). Global primary production: a remote sensing approach. Journal of Biogeograhy. 22(4), 815–835.

Quéré, C.Le., R. Moriarty, R.M. Andrew, J.G. Canadell, S. Sitch, J.I. Korsbakken, P. Friedlingstein, G.P. Peters, R.J. Andres …et al. (2015). Global Carbon Budget 2015. Earth System and Science Data. 7, 349-396.

Redowan, M., R. Akter, M. Islam and K. M. Masum (2015). Estimating growing stock volume in a Bangladesh forest site using Landsat TM and field-measured data, 6(2), 1607–1619.

Richardson, A.J. and C.L. Wiegand (1977). Distinguishing vegetation from soil background information, Photogrammetric Engineering and Remote Sensing, 43(12), 1541-1552.

Running, S.W., P.E. Thornton, R.R. Nemani, J.M. Glassy (2000). Global terrestrial gross and net primary productivity from the earth observing system. pp. 44–57. In Sala O, Jackson R, Mooney H, eds. Methods in Ecosystem Science. New York: Springer-Verlag.

Treitz, P. and J. Rogan (2004). Remote sensing for mapping and monitoring land-cover and land-use change- an introduction. Progress in planning, 61(4), 269-279.

Ullah, S., Y. Si, M. Schlerf, A. K. Skidmore and M. Shafique (2012). Estimation of grassland biomass and nitrogen using MERIS data International Journal of Applied Earth Observation, 19, 196–204.

Walkley, A. and I. A. Black (1934). An examination of Degtjareff method for determining soil organic matter and a proposed modification of the chromic acid titration method. Soil Science, 37, 29-37.

Xue, J., and B. Su (2017). Significant remote sensing vegetation indices: A review of developments and applications. Journal of Sensors, 2017.

Zhou, G. (2014). Determination of green aboveground biomass in desert steppe using litter-soil-adjusted vegetation index. European Journal of Remote Sensing, 47(1), 611–625.

Appendix-I: Species-specific equation used in present study (Source: FSI 1996)

Tree species	Volume eq. used
Abies densa	V=0.10744-2.09529*D+12.62008*D^2-1.61065*D^3
Acer accuminatum	SQRTV=-0.162945+3.109717*D
Acer sp.	SQRTV=-0.162945+3.109717*D
Acer caudatum	SQRTV=-0.162945+3.109717*D
Acer hookeri	SQRTV=-0.162945+3.109717*D
Alnus sp.	V=0.01115-0.11716*D+7.11672*D^2-4.54544*D^3
Alnus nepalenis	V=0.01115-0.11716*D+7.11672*D^2-4.54544*D^3
Alnus nitida	V=0.01115-0.11716*D+7.11672*D^2-4.54544*D^3
Altingia excelsa	V=0.09164-1.21122*D+7.76693*D^2+2.17361*D^3
Betula alnoides	V=0.15958-1.57976*D+8.25014*D^2-0.48518*D^3
Bombax ceiba	V=-0.10513+0.28329*D+6.11575*D^2
Castanopsis sp.	V=0.05331-0.87098*D+6.52533*D^2+1.74231*D^3
Chukrasia tabularis	V=-0.07559+9.23051*D^2
Cinnamomum bejolghota	V=-0.13819+2.28497*D-4.27569*D^2+11.3422*D^3
Cinnamomum camphora	V=-0.13819+2.28497*D-4.27569*D^2+11.3422*D^3
Cinnamomum tamala	V=0.1097-0.88668*D+6.097*D^2-1.62672*D^3
Cinnamomun cecidephne	V=-0.13819+2.28497*D-4.27569*D^2+11.3422*D^3
Citrus sinensis	V=0.15958-1.57976*D+8.25014*D^2-0.48518*D^3
Cyathea sp.	V=0.15958-1.57976*D+8.25014*D^2-0.48518*D^3
Cyperus torulosa	V=0.15958-1.57976*D+8.25014*D^2-0.48518*D^3
Debregeasia longifolia	V=0.15958-1.57976*D+8.25014*D^2-0.48518*D^3
Duabanga grandiflora	SQRTV=-0.05931+2.63098*D
Elaeocarpus rugosus	V=0.15958-1.57976*D+8.25014*D^2-0.48518*D^3
Elaeocarpus sp.	SQRTV=0.43483+5.72522*D-2.59907*SQRTD
Exbuclandia populnea	V=0.15958-1.57976*D+8.25014*D^2-0.48518*D^3
Ficus sp.	SQRTV=0.03629+3.95389*D-0.84421*SQRTD
Ficus auriculata	SQRTV=0.03629+3.95389*D-0.84421*SQRTD
Garcinia sp.	V=0.15958-1.57976*D+8.25014*D^2-0.48518*D^3
Gynocardia odorata	V=0.15958-1.57976*D+8.25014*D^2-0.48518*D^3
Irvingia gabonensis	V=0.15958-1.57976*D+8.25014*D^2-0.48518*D^3
Ligustrum robustum	V=0.15958-1.57976*D+8.25014*D^2-0.48518*D^3
Litchi sineisis	V=0.15958-1.57976*D+8.25014*D^2-0.48518*D^3
Lithocarpus sp.	V=0.15958-1.57976*D+8.25014*D^2-0.48518*D^3
Litsea monopetala	V=0.15958-1.57976*D+8.25014*D^2-0.48518*D^3
Maesa sp.	V=0.15958-1.57976*D+8.25014*D^2-0.48518*D^3
Magnolia campbelli	V=0.15958-1.57976*D+8.25014*D^2-0.48518*D^3
Magnolia sp.	V=0.15958-1.57976*D+8.25014*D^2-0.48518*D^3
Magnolia hodgsonii	V=0.15958-1.57976*D+8.25014*D^2-0.48518*D^3
Mahonia nepalensis	V=0.15958-1.57976*D+8.25014*D^2-0.48518*D^3
Mallotus sp.	V=0.14749-2.87503*D+19.61977*D^2-19.11630*D^3
Mangifera sylvatica	V=0.15958-1.57976*D+8.25014*D^2-0.48518*D^3
Michelia champaca	V=-0.11391+1.06784*D+5.36178*D^2

Michelia doltsopa	V=-0.11391+1.06784*D+5.36178*D^2
Michelia/magnolia oblonga	V=-0.11391+1.06784*D+5.36178*D^2
Moras alba	V=0.15958-1.57976*D+8.25014*D^2-0.48518*D^3
Myrica esculenta	V=0.15958-1.57976*D+8.25014*D^2-0.48518*D^3
Neolitsea zeylanica	V=0.15958-1.57976*D+8.25014*D^2-0.48518*D^3
Neolitsea pulcherima	V=0.15958-1.57976*D+8.25014*D^2-0.48518*D^3
Persea sp.	V=0.15958-1.57976*D+8.25014*D^2-0.48518*D^3
Phoebe pallida	V=-0.0432+0.3622*D^2H
Phoebe lanceolata	V=-0.0432+0.3622*D^2H
Phoenix sp.	V=0.15958-1.57976*D+8.25014*D^2-0.48518*D^3
Pinus wallichiana	V=0.22736-0.027394*D3+0.0012413*D^2(dia in cm)
Pinus roxburgii	V=0.22736-0.027394*D3+0.0012413*D^2(dia in cm)
Prunus sp.	V=0.15958-1.57976*D+8.25014*D^2-0.48518*D^3
Prunus nepalensis	V=0.15958-1.57976*D+8.25014*D^2-0.48518*D^3
Prunus persica	V=0.15958-1.57976*D+8.25014*D^2-0.48518*D^3
Pyrus sp.	V=0.15958-1.57976*D+8.25014*D^2-0.48518*D^3
Quercus dealbata	V=-0.04378+6.2342*D^2
Quercus glauca	V=-0.04378+6.2342*D^2
Quercus myrsinifolia	V=-0.04378+6.2342*D^2
Quercus lamellosa	V=-0.04378+6.2342*D^2
Quercus semiserrata	V=-0.04378+6.2342*D^2
Rhododendron hodgsonii	V=-0.08934+0.7073*D+2.13941*D^2
Rhododendron grande	V=-0.08934+0.7073*D+2.13941*D^2
Rhododendron dalhousiae	V=-0.08934+0.7073*D+2.13941*D^2
Rhododendron coxianum	V=-0.08934+0.7073*D+2.13941*D^2
Rhododendron subansirians	V=-0.08934+0.7073*D+2.13941*D^2
Rhododendron boothii	V=-0.08934+0.7073*D+2.13941*D^2
Rhododendron falconeri	V=-0.08934+0.7073*D+2.13941*D^2
Rhododendron kendrickii	V=-0.08934+0.7073*D+2.13941*D^2
Salvadora persica	V=0.15958-1.57976*D+8.25014*D^2-0.48518*D^3
Sapium buccatum	V=0.15958-1.57976*D+8.25014*D^2-0.48518*D^3
Saurauia nepalensis	V=0.15958-1.57976*D+8.25014*D^2-0.48518*D^3
Schima sp.	V=0.15958-1.57976*D+8.25014*D^2-0.48518*D^3
Schima wallichii	V=0.15958-1.57976*D+8.25014*D^2-0.48518*D^3
Symplocos theifolia	V=0.15958-1.57976*D+8.25014*D^2-0.48518*D^3
Taxus wallichiana	V=0.15958-1.57976*D+8.25014*D^2-0.48518*D^3
Toona ciliata	V=0.21869-2.04074*D+10.41713*D^2+1.85232*D^3
Trema orientalis	V=0.15958-1.57976*D+8.25014*D^2-0.48518*D^3
Tsuga dumosa	SQRTV=-0.09154+2.37257*D